

Conduction and Hall measurements of $\text{Ba}_2\text{YCu}_3\text{O}_{6+\delta}$ films at high temperatures: The role of oxygen

A. Davidson, P. Santhanam, A. Palevski, and M. J. Brady

IBM Research Division, Thomas J. Watson Research Center, P.O. Box 218, Yorktown Heights, New York 10598

(Received 1 February 1988; revised manuscript received 18 April 1988)

We report new resistance and Hall effect measurements for $\text{Ba}_2\text{YCu}_3\text{O}_{6+\delta}$. The data were taken at temperatures up to 1100 K, and at various oxygen partial pressures. For $T > 700$ K, the resistivity shows an activated temperature dependence, and a square-root pressure dependence. Measurements of oxygen content in the literature, however, show a dependence on pressure that is much weaker than square root. For the measurements of resistivity and oxygen content to be consistent, the mechanism for conduction at high temperatures is likely to be hopping. Our experiments are the first to show that the linear temperature dependence of the effective Hall carrier density persists up to ≈ 700 K and then drops.

Superconductivity in the new high-transition-temperature oxides cannot be fully understood without an explanation of the normal-state conduction mechanism. By measuring transport properties over a wide temperature range, we are able to begin building a model for conduction in $\text{Ba}_2\text{YCu}_3\text{O}_{6+\delta}$. Reports on high-temperature transport in the literature are mainly on bulk samples. Freitas and Plaskett have done careful resistivity measurements on bulk ceramics at high temperatures¹ and various oxygen partial pressures, and have proposed a model of normal conduction based on their measurements.² Davidson *et al.*³ have reported similar results on thin films. Fiory, Gurvitch, Cava, and Espinosa⁴ have measured resistance at elevated temperatures in ceramics, with results similar to Freitas and Plaskett.¹ They propose a model for conduction focused primarily on the regime below the orthorhombic-tetragonal (O-T) transition temperature. Ronay⁵ has proposed a model of carrier density, independent of any particular band model, based on the law of mass action. Choi, Tuller, and Tsai⁶ have measured thermopower and resistivity in the bulk at high temperature and proposed a specific defect model to explain their data. The Hall effect in this material has been measured by several workers⁷⁻¹⁰ from room temperature to the superconducting transition in bulk ceramics and in single crystals. In this article, we address the issue of dependence of the resistivity and Hall coefficient on pressure and temperature in thin films. Our interpretation of the resistivity data focuses on the temperature range above the O-T transition (about 900 K), while the Hall data are discussed mainly below 700 K. The use of thin films conveniently assures fast oxygen kinetics, and allows the measurement of the Hall effect in small magnetic fields compatible with high temperatures.

Our samples were deposited by electron-beam coevaporation of the metals onto MgO substrates, as described previously.¹¹ After heat treatment,³ they were superconductive at typically 85 K, with sharp transitions. They were polycrystalline and unoriented. They were approximately 1 μm thick, with large grains and diffuse optical scattering. For resistivity measurements, we used a sample holder with platinum rhodium contacts, suitable for

full insertion into a tube furnace. Mixtures of helium and oxygen gas were piped through the furnace, and exhausted through a thick layer of glass wool, which proved effective in stopping back diffusion of the room atmosphere. The flow rates of the two gases were the order of a few liters per minute, as measured by "floating ball" gauges that had been calibrated by displacing water from an inverted beaker.

Typical resistance data are shown as the solid curves in Fig. 1. At high temperature the resistance increases exponentially, especially at low oxygen pressures. The resistance at low temperatures extrapolates almost to zero at zero Kelvin for high pressures, and approaches a constant value for the lowest pressures. A bump is visible on each curve in the range 700–900 K, that has been shown^{1,3} to correspond to the ordering of the absorbed oxygen into chains, and the concomitant tetragonal-to-orthorhombic phase transition. An Arrhenius plot (not shown) for this transition point agrees very well with the earlier work of

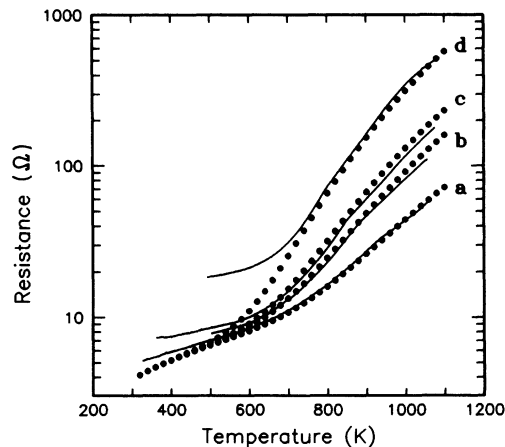


FIG. 1. Semilog plot of resistance vs temperature for 1 μm film on MgO substrate. The four solid lines are data taken at four different values of oxygen partial pressure. Curves a through d are for 1, 0.158, 0.07, and 0.01 atm respectively. The circles are a fit of Eq. (1), as discussed in the text.

Freitas and Plaskett¹ on bulk ceramic samples. This agreement is important because it shows that our samples were in thermodynamic equilibrium for temperatures greater than 700 K.

The circles in Fig. 1 represent a phenomenological fit to the following equation:

$$R = R_0 T + \frac{A}{\sqrt{P}} e^{-H/T}, \quad (1)$$

where R is the resistance in ohms, T the temperature in K, P the oxygen partial pressure in atmospheres, and R_0 , H , and A are fitting parameters. All the curves in the figure were fit with $H=6800$ K, $R_0=0.013$ Ω/K , and $A=22000$ $\Omega - \text{atm}^{1/2}$. Note that R_0 , H , and A were adjusted for a fit to curve *a* in Fig. 1, and the other curves were generated by using measured values of the oxygen pressure P . The dependence of the resistance on \sqrt{P} at high temperature is clearly seen. The linear term on the right-hand side of Eq. (1) has been commonly observed on high quality samples, and has been shown to correspond to conduction in the *a-b* plane of single crystals.⁷ Its origin⁴ is not addressed in this paper. The deviation from linearity in curve *d* at low temperature is due to incomplete oxygen uptake because of the low oxygen pressure. The data of Freitas and Plaskett¹ can be fit very well to Eq. (1) with similar parameters. Choi *et al.*⁶ have reported the \sqrt{P} dependence, but our fit to Eq. (1) makes it particularly clear. We will interpret Eq. (1) later in this article.

Figure 2 graphs the Hall data for another film. The Hall coefficient was measured by extending the furnace tube outside of the oven far enough to be surrounded by a water-cooled solenoid. The sample was heated indirectly by the hot gas flowing through the extended tube. The maximum sample temperature was limited by our ability to cool the solenoid. To get a sample temperature of 600°C, the oven was at 1200°C, and the magnet reached over 100°C at the surface. The flow rates necessary were

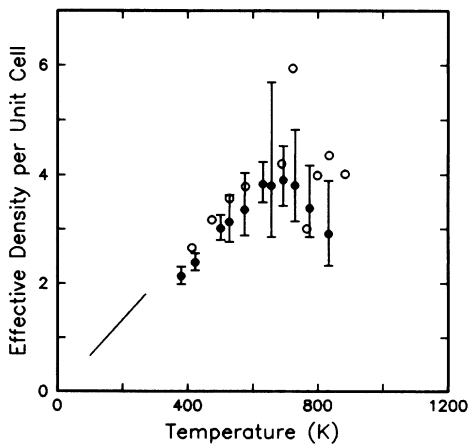


FIG. 2. Effective carrier density per unit cell, from Hall effect data, vs temperature. The line in the lower left represents data from Ref. 8. The open circles were measured in 1 atm oxygen ambient pressure, and the filled circles are for less than about 0.1 atm of ambient oxygen. Error bars for the second case are shown, and error bars for 1 atm were similar.

beyond the calibration of the flow meters. Therefore, for the case when oxygen and helium were mixed (filled circles in Fig. 2), the partial pressure of oxygen is estimated to have been below 0.1 atm.

The electrical contacts were made in a van der Pauw configuration by mechanical pressure maintained with a ceramic jig to four gold balls attached to gold wires. We used a dc sample current, ac magnet current, and the Hall voltage was measured by a lock-in amplifier whose reference channel was driven by a signal proportional to the instantaneous magnet current. We were able to measure nanovolt Hall voltages with mA dc Hall currents in an ac magnetic field of the order of 100 Grms. This represents 6 orders of magnitude discrimination against the resistive voltage developed between the Hall contacts. The magnetoresistance contribution due to the small fields used was negligible. Also the ac field technique would cause any residual magnetoresistance signal to appear at the second harmonic of the reference frequency, while we obtain the Hall voltage at the fundamental. The error bars in the Hall density data are due to the very high sensitivity of the film resistance to temperature and pressure. This sensitivity results in a noise proportional to bias current and to dR/dT , which increases exponentially with temperature. Temperature or pressure fluctuations in the parts per million are enough to account for the noise.

All the data showed conduction to be dominated by holes. The open circles were in equilibrium at 1 atm of flowing oxygen, while the filled circles are data collected at a reduced oxygen pressure. The straight line in the lower left corner represents the results of Penney, Shafer, Olson, and Plaskett⁸ who measured the Hall coefficient at low temperature in bulk ceramic samples. (There is also recent work¹² showing similar behavior at low temperatures in single crystals in the *a-b* plane.) It is observed that our data are a direct continuation of this line showing that the linear temperature dependence of the effective Hall density extends from 100 to about 700 K, and rises almost an order of magnitude over that range. Only at the highest temperature and the lowest oxygen is there clear evidence that the effective carrier concentration begins to diminish. Recent results of Grader, Gallagher, and Fiory¹³ have shown very similar behavior of both the resistivity and Hall effect.

Now we would like to draw attention to the essential features of the resistance and Hall data. (1) The exponential term in Eq. (1) that fits the resistance data at high temperature has a prefactor that depends on the square root of the oxygen gas partial pressure. (2) The energy factor $H=6800$ K in Eq. (1) fits *all* the curves to within experimental error. In other words, taking H independent of temperature and pressure is sufficient to explain our data. (3) The effective Hall density ceases its linear rise at about 700 K, which is the temperature at which the oxygen begins to leave the lattice. The drop in Hall density about 700 K is reasonable evidence that carriers are removed as oxygen is removed, which suggests a semiconductorlike picture with the oxygen acting as dopant.

Features (1) and (2) discussed in the last paragraph could be explained in either a conventional semiconductor

model, or a hoppinglike model. The semiconductor model is basically contained in the following equations:

$$\delta \propto \sqrt{P} e^{H_s/T}, \quad (2a)$$

$$\sigma \propto \delta e^{-E_g/2T} \propto \sqrt{P} e^{[H_s - (E_g/2)]/T}. \quad (2b)$$

Here, δ is the oxygen concentration, as defined in the chemical formula $\text{Ba}_2\text{YCu}_3\text{O}_{6+\delta}$, and σ is the electrical conductivity. Equation (2a) is Sievert's law,¹⁴ governing the absorption of a diatomic gas into the solid in the dilute limit. If the absorbed oxygens act as dopants, and the dopants are separated from a band edge by energy E_g , then we would expect Eq. (2b) to describe the conductivity. To fit the data we need $H_s - (E_g/2) = 6800$ K. According to Bakker, Welch, and Lazareth,¹⁵ and confirmed by Freitas and Plaskett,¹ $H_s = 11\,600$ K, so that $E_g = 9600$ K. Although this simple model explains several aspects of the high-temperature data, it disagrees with experimental measurements that show much weaker dependence of oxygen content on T and P than is required by Eq. (2a).

In the hoppinglike model we use the following equations:

$$\frac{\delta}{1-\delta} = (0.00214)(P^{1/4})(e^{(H_s/2T)}), \quad (3a)$$

$$\sigma \propto \left(\frac{\delta}{1-\delta} \right)^2 e^{-\epsilon/T} \propto \sqrt{P} e^{(H_s - \epsilon)/T}. \quad (3b)$$

Equation (3a) is a phenomenological fit to experimental results, with a particularly weak dependence of δ on P . The specific form of this equation is discussed below. In order for the conductivity to agree with Eq. (1), we require a very strong dependence on δ , as we have put into the prefactor in Eq. (3b). We note that the δ dependence in Eq. (3b) is much stronger than a simple exponential. This behavior is reminiscent of the exponential dependence of resistivity on dopant concentration in impurity conduction in semiconductors,¹⁶ where the mechanism is known to be hopping. To obtain fits in the model and reproduce Eq. (1), we have used $H_s = 13\,500$ K, and $\epsilon = 6700$ K for the hopping activation energy. We suppose that in $\text{Ba}_2\text{YCu}_3\text{O}_{6+\delta}$ charge carriers are coupled from the absorbed oxygens into the two-dimensional copper-oxygen planes, where they conduct at high temperature by hopping. With sufficient doping and structural modifications,¹⁷ there is a transition to a metallic behavior.

Both the semiconductor model in Eq. (2) and the hoppinglike model in Eq. (3) are consistent with the data represented by Eq. (1). However, the two models make different assumptions about the influence of pressure and temperature on the oxygen content δ . The semiconductor model requires a strong dependence of δ on T and P , while the hopping picture is consistent with weak dependences. These two cases can, in principle, be distinguished by independent measurements of the oxygen content.

There have been several such independent measurements of δ using thermogravimetric analysis^{18,19} (TGA) neutron diffraction,²⁰ and titration²¹ techniques. Although there are discrepancies in detail among these results, they all show weak T and P influence, which is phenomenologically described Eq. (3a). This is shown in Fig.

3, which plots the TGA data of McKinnon *et al.*¹⁹ along with the solution for δ of Eq. (3a). The parameters in Eq. (3a) were chosen to fit the curve for 1 atm and the other curve was generated by using the measured partial pressure. It is worth noting here that Eqs. (2a) and (3a) are both consistent with a linear Arrhenius plot, as discussed by Freitas and Plaskett,¹ with similar values of H_s .

The observed weak influence of T and P on oxygen content, then, tends to favor the hoppinglike model. For the simple doped semiconductor picture to prevail, the oxygen content measurements would have to be wrong, perhaps due to a nonequilibrium situation.

The main feature to be explained in the Hall data is the linear temperature dependence of effective density over almost a decade in temperature. That is, we have both $\sigma \propto 1/T$ and $R_H \propto 1/T$ at the same time, and the Hall mobility $\mu_H = \sigma R_H \propto 1/T^2$. As noted by Penney⁸ and others such behavior is difficult to get within a single band model for a metal, so we want to see if two bands could account for it by the mechanism of compensation. The idea of compensation is that neither band should dominate the Hall coefficient R_H . Therefore, in this model, the two bands should be fairly symmetric, with comparable densities and mobilities over the whole range of $1/T$ behavior. Let us assume that below 700 K the carrier densities are constant and equal, and see if the data can be still reasonably explained. Under these conditions the simple isotropic two-band Hall coefficient becomes

$$R_H = \frac{\mu_h - \mu_e}{n e (\mu_h + \mu_e)} = \frac{\mu_h - \mu_e}{\sigma}, \quad (4)$$

where n is the carrier density of each band, and μ_e and μ_h are the electron and hole mobilities, respectively. We find then that both the resistivity data and the Hall data can be satisfied if the mobilities are dominated by the initial terms of a Taylor expansion in $1/T$. That is $\mu_h = c_0/T(1 + c_1/T)$ and $\mu_e = c_0/T(1 - c_1/T)$, where c_0 and c_1 are constants. Substitution of μ_h and μ_e in Eq. (4)

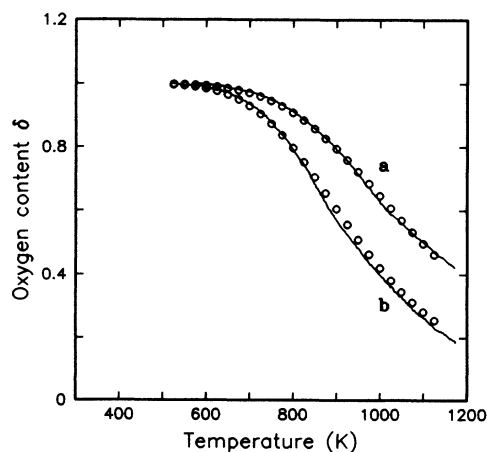


FIG. 3. Comparison of the TGA data (lines, Ref. 19) to the solution of Eq. (3a) for δ (circles). Curves *a* and *b* are for 1.0 and 0.025 atm, respectively. Parameters were adjusted to fit curve *a* and changing only the pressure according to its measured value was sufficient to fit curve *b*.

yields $\mu_H = \sigma R_H = \mu_p - \mu_n \propto 1/T^2$, as required above.

Although this interpretation of the mobilities hinges on the use of Eq. (4), which is of limited validity, the general idea of compensation will require two bands with rather symmetric properties. Even a more detailed theory²² accounting for granularity and anisotropy will require this symmetry.

In summary, we report resistivity on thin films of $\text{Ba}_2\text{YCu}_3\text{O}_{6+\delta}$ at temperatures up to 1100 K and Hall measurements up to 900 K at various partial pressures of oxygen. To fit the weak pressure and temperature dependence of the oxygen content (reported in the literature), we propose a phenomenological equation [Eq. (3a)] consistent with the thermodynamic observations of Freitas and Plaskett.¹ However, we then observe that the conductivity at high temperature has too strong of a dependence on pressure and temperature for the carrier density to be simply proportional to oxygen content. Since it is difficult to imagine a process for the influence of conductivity by pressure except through changes in oxygen concentration,

the conductivity needs a mechanism that is strongly influenced by the oxygen. We conjecture that this mechanism has to do with wave-function overlaps in the copper-oxygen sheets, similar to the known behavior of impurity bands in doped semiconductors. We have also observed that the linear temperature dependence of the effective Hall density persists up to 700 K, and then drops as oxygen is removed. The strong pressure dependence of the resistivity above 700 K and the linear temperature dependence of the Hall density below 700 K are two major features to be explained by transport theories of this material.

Films were provided by R. B. Laibowitz. W. R. McKinnon provided the digitized data for oxygen content used in Fig. 3. Important discussions were held with T. Plaskett, P. Freitas, D. Goldschmidt, V. Moruzzi, M. Shafer, I. Haller, T. Penney, A. Kleinsasser, and W. J. Gallagher.

¹P. P. Freitas and T. S. Plaskett, Phys. Rev. B **36**, 5723 (1987).

²P. P. Freitas and T. S. Plaskett, Phys. Rev. B **37**, 3657 (1988).

³A. Davidson, A. Palevski, M. J. Brady, R. B. Laibowitz, R. Koch, M. Scheuermann, and C. C. Chi, Appl. Phys. Lett. **52**, 157 (1988).

⁴A. T. Fiory, M. Gurvitch, R. J. Cava, and G. P. Espinosa, Phys. Rev. B **36**, 7262 (1987).

⁵M. Ronay, Phys. Rev. B **36**, 8860 (1987).

⁶G. M. Choi, H. L. Tuller, and M.-J. Tsai, in *High Temperature Superconductors*, edited by Merwyn B. Brodsky, Robert C. Dynes, Koichi Kitawawa, and Harry L. Tuller, Materials Research Society Symposium Proceedings, Vol. 99 (Materials Research Society, Pittsburgh, 1988), p. 141.

⁷S. W. Tozer, A. W. Kleinsasser, T. Penney, D. Kaiser, and F. Holtzberg, Phys. Rev. Lett. **59**, 1768 (1987).

⁸T. Penney, M. W. Shafer, B. L. Olson, and T. S. Plaskett, Adv. Ceram. Mater. **2**, 577 (1987).

⁹N. P. Ong, Z. Z. Wang, J. Clayhold, J. M. Tarascon, L. H. Greene, and W. R. McKinnon (unpublished).

¹⁰Duan Hong-min, Lu Li, Wang Xie-mei, Lin Shuyuan, and Zhang Dian-lin, Solid State Commun. **64**, 489 (1987).

¹¹R. B. Laibowitz, R. H. Koch, P. Chaudhari, and R. J. Gambi-

no, Phys. Rev. Lett. **58**, 2687 (1987).

¹²T. Penney (private communication).

¹³G. S. Grader, P. K. Gallagher, and A. T. Fiory, Phys. Rev. B **38**, 844 (1988).

¹⁴L. D. Landau and E. M. Lifshitz, *Statistical Physics, Part I* (Pergamon, New York, 1980), pp. 271 and 310.

¹⁵H. Bakker, D. O. Welch, and O. W. Lazareth, Jr., Solid State Commun. **64** 237 (1987).

¹⁶B. I. Shklovskii and A. L. Efros, *Electronic Properties of Doped Semiconductors* (Springer-Verlag, New York, 1984), p. 78.

¹⁷R. J. Cava, Bull. Am. Phys. Soc. **33**, 212 (1988).

¹⁸P. K. Gallagher, Adv. Ceram. Mater. **2**, 632 (1987).

¹⁹W. R. McKinnon, M. L. Post, L. S. Selwyn, G. Pleizier, J. M. Tarascon, P. Barboux, L. H. Greene, and G. W. Hull (unpublished).

²⁰M. A. Beno, L. Soderholm, D. W. Capone II, D. G. Hinks, J. D. Jorgensen, J. D. Grace, Ivan K. Schuller, C. U. Segre, and K. Zhang, Appl. Phys. Lett. **51**, 57 (1987).

²¹M. W. Shafer, T. Penney, and B. L. Olson, Phys. Rev. B **36**, 4047 (1987).

²²Ting-Kang Xia and D. Stroud, Phys. Rev. B **37**, 118 (1988).